

Vortex-chain state in $\text{Bi}_2\text{Sr}_2\text{CaCu}_2\text{O}_{8+\delta}$: Experimental evidence for coexistence of two vortex orientations

I. V. Grigorieva and J. W. Steeds

Physics Department, University of Bristol, Bristol BS8 1TL, United Kingdom

G. Balakrishnan and D. M. Paul

Physics Department, University of Warwick, Coventry CV4 7AL, United Kingdom

(Received 17 October 1994)

A detailed study is reported by the Bitter decoration technique of the mixed vortex chain-vortex lattice phase found in tilted magnetic fields in single crystals of the highly anisotropic $\text{Bi}_2\text{Sr}_2\text{CaCu}_2\text{O}_{8+x}$ (BSCCO). From the field and tilt-angle dependencies of the vortex periods in this structure we conclude that the vortex chains in BSCCO are qualitatively different from those in the moderately anisotropic and well-studied $\text{YBa}_2\text{Cu}_3\text{O}_x$. In particular, the intrachain vortex period is independent of the tilt angle φ for a given perpendicular component of the field while the vortex period in the intervening flux-line lattice (FLL) shows a maximum vs φ . In addition, the ratio of the number of the FLL vortices to the total number of vortices decreases rapidly for $\varphi > 70^\circ$. Proceeding from these dependencies, we show that the observed mixed vortex phase can be explained consistently by the chain and the FLL vortices having different orientations, neither parallel to the applied field, as suggested by recent theoretical calculations.

INTRODUCTION

It is now well established that the phase diagram of the mixed state in copper-oxide superconductors is characterized by a variety of vortex phases that replace each other depending on temperature, magnetic field, and orientation of the magnetic field. In the low-field region, for an external field applied at an oblique angle relative to the anisotropy axis c , the usual isotropic flux-line lattice (FLL) should transform into a uniaxially distorted hexagonal lattice oriented symmetrically about the tilt plane¹ (the latter is the plane containing the direction of the external field \mathbf{B}_{ext} and the c axis). Furthermore, as a result of the weak coupling between the superconducting CuO_2 planes, the character of the intervortex interaction at large tilt angles changes from the usual repulsion to attraction within the tilt plane. This, in turn, leads to the formation of the so-called vortex chains.²⁻⁵ The vortex-chain phase was predicted within the framework of anisotropic London theory²⁻⁴ and later observed directly in Y-Ba-Cu-O single crystals by Bitter decoration experiments.^{6,7}

Recently, an even more complicated phenomenon in tilted magnetic fields has been considered,⁸⁻¹¹ that is a possibility of the coexistence of different vortex "species." For superconductors with extreme anisotropies, like $\text{Bi}_2\text{Sr}_2\text{CaCu}_2\text{O}_{8+\delta}$ (BSCCO), it was found that within a certain interval of tilt angles the FLL uniformly tilted and parallel to the external field may become unstable and be replaced by two coexisting vortex species having different orientations in the bulk of a superconductor: one parallel to the c axis and the other parallel to the (ab) plane,⁸ or one parallel to the c axis and the other parallel to the external field,⁹ or both tilted further away from the c axis in comparison with \mathbf{B}_{ext} but not parallel to the (ab) plane.^{10,11} The last situation is predicted to occur as a

result of having, at low fields, two minima in the Gibbs free energy of the FLL, which for certain values of the anisotropy parameter, $\gamma = (m_c/m_{ab})^{1/2}$, and Ginzburg-Landau (GL) parameter, κ , can be degenerate¹⁰ [here m_c and m_{ab} are the effective masses along the c axis and in the (ab) plane, respectively]. The above theories have been put forward, in particular, as attempts to explain a vortex structure observed by the Bitter decoration in highly anisotropic BSCCO for tilt angles $\varphi \geq 60^\circ$.¹² The structure consisted of dense vortex chains running roughly parallel to the tilt plane which coexisted with the intervening isotropic vortex lattice. The theories suggested that in the case of two coexisting vortex orientations, vortices of one orientation could have been attracted to each other and thus formed the vortex chains, while vortices of the other orientation only interacted via magnetic repulsion and formed the intervening FLL. Alternatively, it was suggested¹³ that the two formed two sets of vortex chains, with different equilibrium vortex spacings. However, neither of these scenarios by themselves suffice to explain the existing experimental data on BSCCO, in particular, the field and tilt-angle dependencies of the vortex spacings in the observed structure. The chief characteristics of the phase with attraction-driven vortex chains are the nontrivial dependencies of the intrachain vortex period a_{ch} on applied field and tilt angle. Within the framework of anisotropic London theory it was found that a_{ch} should be independent of the applied field and change nonmonotonically with tilt angle, exhibiting a minimum at around 70° tilt. This behavior was indeed observed in both pure⁶ and Al-doped $\text{YBa}_2\text{Cu}_3\text{O}_7$ (YBCO) crystals.⁷ However, in BSCCO, evolution of the chain-FLL mixture with applied field appeared to contradict both the theory and the behavior observed in the moderately anisotropic YBCO, since all the vortex periods (in the chains, between the chains and in the in-

tervening FLL) were found to change approximately as $\propto 1/\sqrt{B_z}$ (where B_z is the normal component of the applied field).¹² At the same time, no clear dependencies of these parameters on tilt angle were reported.

In the present paper we report a detailed study by the Bitter decoration technique of the mixed vortex-chain-FLL phase in BSCCO single crystals. We have focused on the dependence of the chain and FLL parameters on tilt angle φ and the applied field. Due to very high quality and homogeneity of the single crystals used in this study, we were able to reveal systematic changes in the vortex structure with tilt angle that clearly indicated its anisotropy-related origin. We find that neither the field, nor the tilt-angle dependencies of the chain and FLL parameters can be simply accounted for by the anisotropy-induced intervortex attraction as the mechanism responsible for the formation of the vortex-chain-FLL mixture. In particular, we find that, for a given B_z , the intrachain vortex period a_{ch} is independent of tilt angle, while a_{FLL} and the ratio a_{FLL}/a_{ch} (a_{FLL} is the FLL period) show nonmonotonic dependencies on φ . In addition, we find a rapid growth of the ratio of the chain vortices to the total number of vortices in the structure for $\varphi > 70^\circ$. Proceeding from these findings, we demonstrate that the vortex-chain phase in BSCCO can be understood consistently if one assumes that both the chain and FLL vortices are parallel neither to the direction of the applied field, nor to the crystallographic axes, as suggested in Refs. 10 and 11. Our studies of less homogeneous samples revealed that even relatively weak pinning causes substantial spread of the chain and FLL parameters thus smearing out the above dependencies.

EXPERIMENTAL RESULTS AND DISCUSSION

Single crystals of BSCCO-2212 composition ($\text{Bi}_2\text{Sr}_2\text{CaCu}_2\text{O}_{8+\delta}$) were grown by the floating-zone method using a double ellipsoidal infrared image furnace, as described in Ref. 14. The crystals exhibited sharp superconducting transitions at $T_c = 92\text{--}93$ K and had standard crystallography, with the c axis along the shortest dimension of the crystal. The high T_c 's and very high quality of the crystals are believed to arise from the optimum stoichiometry of oxygen achieved as a result of striking the right conditions for crystal growth. The Bitter decoration technique is now a standard method used by several groups (see, for example, Refs. 6, 7, 12, and 15). Decorations were performed on as-grown crystals at 4.2 K, after field cooling in the magnetic field applied at an oblique angle to the sample surface. Prior to decoration, the crystals were cleaved so that fresh surfaces parallel to the (ab) planes were exposed. After that, typical sizes of the samples were $2 \times 2 \times (0.02\text{--}0.05)$ mm³. The tilt angle φ (the angle between the c axis of the sample and the applied field) measured with the accuracy of $\pm 0.5^\circ$ was varied between 0 and 87° . The external field B_{ext} measured by the Hall probe, was varied between 20 and 150 Oe. Two or three crystals were decorated simultaneously in every experiment (i.e., at the same φ and B_{ext}), so that it was possible to compare data obtained in identical circumstances on different crystals. More than

40 samples were studied altogether. Two typical decoration images of the vortex-chain-FLL mixture obtained in the scanning electron microscope (SEM) are shown in Fig. 1. Essential features of the vortex phase studied here are obvious in these two images. Both the vortex chains and the intervening FLL are well ordered; the chains orientated parallel to the (\mathbf{B}, \mathbf{c}) plane are fairly straight and the ordering of the FLL is mainly interrupted by the presence of the denser vortex chains. [In less homogeneous samples which we will not consider here, the chains go up and down and often deviate substantially from the (\mathbf{B}, \mathbf{c}) plane projection; in addition, the FLL between the chains in such samples is rather disordered.]

Our measurements of the vortex-chain and FLL parameters versus field and tilt angle revealed a number of new features. Figure 2 shows the dependence of the average magnetic induction at the sample surface B_{obs} on φ . The magnetic induction was calculated from the average vortex density over large areas containing many vortex

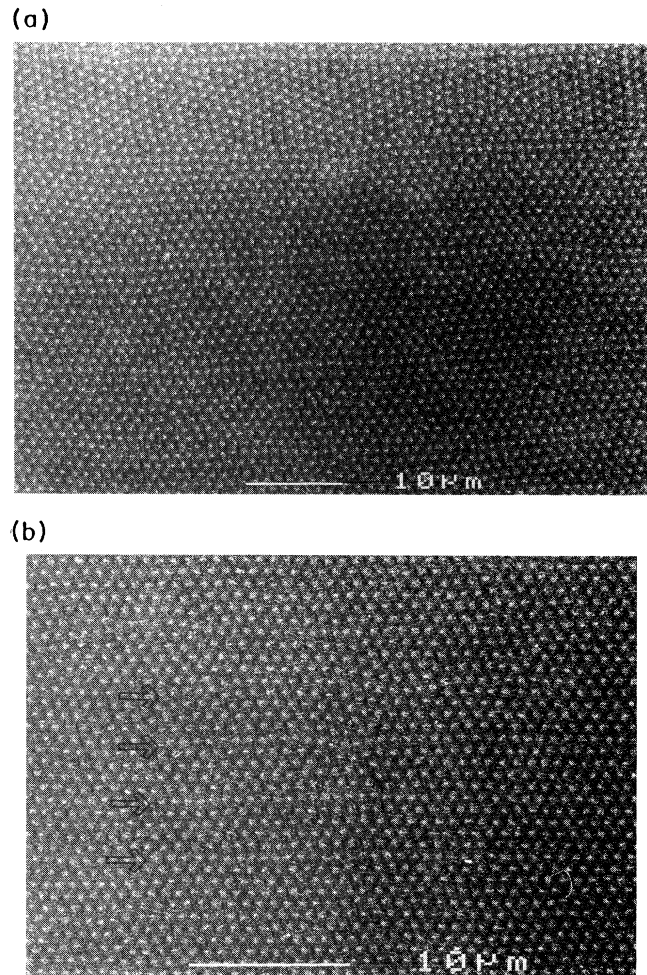


FIG. 1. SEM images of the mixed vortex-chain-FLL phase. (a) The tilt angle of the external field $\varphi = 60^\circ$. (b) $\varphi = 80^\circ$. The projections of the (\mathbf{B}, \mathbf{c}) plane on the sample surface are horizontal. Since the vortex chains in Fig. 1(b) are not seen very easily, few of them are marked by the arrows.

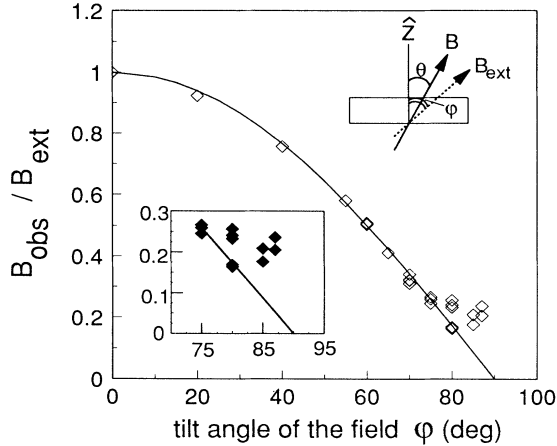


FIG. 2. The ratio of the average magnetic induction measured at the sample surface B_{obs} to the external field B_{ext} vs the tilt angle of B_{ext} . The solid line is $\cos\varphi$ vs φ dependence. The lower inset shows an enlarged view of the data for the largest tilt angles.

chains as $B_{\text{obs}} = N \cdot \Phi_0 / S$ (N is the number of vortices over the area S , Φ_0 is the flux quantum). One can see that for $\varphi < 80^\circ$, $B_{\text{obs}} = B_{\text{ext}} \cos\varphi \equiv B_z$, i.e., the average vortex density is determined by the perpendicular component of the external field B_z as is usual in decoration experiments in tilted fields.^{6,7,12,15} However, for the largest tilt angles, $\varphi = 85$ and 87° , B_{obs} is considerably larger than $B_z \equiv B_{\text{ext}} \cos\varphi$. Namely, at $\varphi = 85^\circ$, B_{obs} is more than twice larger than B_z and at $\varphi = 87^\circ$, it exceeds B_z by five times. The difference ($B_{\text{obs}} - B_z$) is found to be an intrinsic, sample-dependent property which is not noticeably sensitive to other parameters, such as the thickness of the crystal. For $\varphi = 80^\circ$, it was found that four out of seven samples studied, exhibited $B_{\text{obs}} \approx B_z$; however, for the other three samples, $B_{\text{obs}} > B_z$ was found. In order to check the dependence of ($B_{\text{obs}} - B_z$) on the sample thickness (i.e., on the demagnetization factor) we decorated in the same experiment a thick, $\approx 80\text{-}\mu\text{m}$ crystal and a thin, $\approx 20\text{-}\mu\text{m}$ slice of the same crystal cleaved just before the decoration. The two always exhibited the same difference ($B_{\text{obs}} - B_z$), while variations between different crystals could be substantial. Implications of this effect will be discussed later. Note that the values of the external field B_{ext} in Fig. 2 and other plots are given with account taken of the magnetic-flux expulsion during the sample cooling (Meissner effect). The Meissner fractions for our samples and fields were typically between 5 and 15%. In order to measure the expulsion of the perpendicular field component (which defines the average vortex density at the surface), additional samples, mounted with their c axes parallel to the field, were decorated simultaneously with the tilted ones. They had similar dimensions with the tilted crystals, i.e., the same demagnetization factors, and were of similar quality.

The magnetic-field dependencies of a_{ch} and a_{FLL} were studied for $\varphi = 70$ and 80° . For $\varphi = 70^\circ$, both vortex

periods change as $\propto 1/\sqrt{B_z}$. The distance between the vortex chains D_{ch} also decreases as $\propto 1/\sqrt{B_z}$, i.e., for a given tilt angle, the average number of the vortex rows “locked” between the chains remains constant. The same inverse square-root field dependence is found for $\varphi \geq 80^\circ$ but in those cases B_z should be replaced by B_{obs} , i.e., a_{ch} , a_{FLL} , $D_{\text{ch}} \propto 1/\sqrt{B_{\text{obs}}}$.

On changing the tilt angle φ we have also found systematic changes in a_{ch} , a_{FLL} , and D_{ch} , which undoubtedly point to the anisotropy-related origin of the chain-FLL structure but are strikingly different from the behavior of the attraction-driven vortex chains in YBCO. The results are summarized in Fig. 3. First, for a given value of the perpendicular field component, a_{ch} is independent of φ (at $\varphi \geq 80^\circ$ $B_{\text{ext}} \cos\varphi$ should be replaced by B_{obs} , as above). Second, the FLL period a_{FLL} changes nonmonotonically with φ . As a result, the $a_{\text{FLL}}/a_{\text{ch}}$ ratio shows a pronounced maximum at $70\text{--}75^\circ$ tilt. Plotting the ratio of $a_{\text{FLL}}/a_{\text{ch}}$, rather than individual values of a_{ch} and a_{FLL} , in Fig. 3(a) allowed us to include data for different sam-

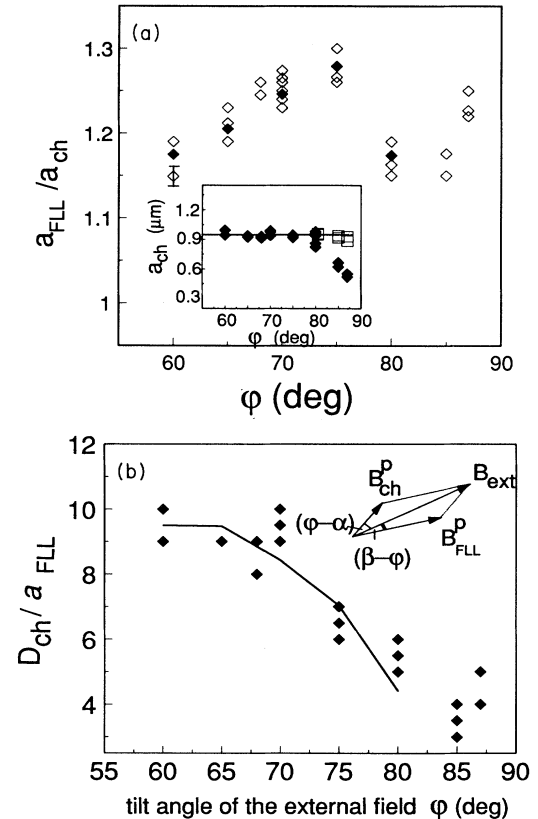


FIG. 3. Evolution of the parameters of the observed vortex structure with tilt angle. (a) The ratio of the FLL vortex period a_{FLL} to the intrachain vortex period a_{ch} vs φ . Each symbol corresponds to a different crystal. Filled symbols show the data used for calculations of $D_{\text{ch}}/a_{\text{FLL}}$ (see text). The inset shows the intrachain vortex period vs φ : \blacklozenge for $B_{\text{ext}} \cos\varphi = 20$ G; \square , for $B_{\text{obs}} = 20$ G. (b) The number of the FLL vortex rows locked between the chains vs φ . The solid line shows the results of calculations using expression (4)—see text.

ples obtained in different applied fields (every symbol in the plot corresponds to a new sample). Deviations of the parameters within the same sample are indicated by the error bar. An upturn of the $a_{\text{FLL}}/a_{\text{ch}}$ (φ) curve is observed for the largest tilt angles, 85 and 87°.

Figure 3(b) shows typical numbers of the FLL vortex rows locked between the chains $D_{\text{ch}}/a_{\text{FLL}}$ versus φ . It should be noted that ± 1 deviations from the values shown could be usually found for each sample but the proportion of these deviations was always small and did not make a significant contribution to the average. One can see that the ratio $D_{\text{ch}}/a_{\text{FLL}}$ decreases rapidly and monotonically, reaching at $\varphi=80^\circ$ roughly half of its value at $\varphi=60^\circ$. This change is also obvious from comparison of the two decoration images in Fig. 1. For the largest tilt angle 87°, $D_{\text{ch}}/a_{\text{FLL}}$ shows a slight upturn, just like the ratio $a_{\text{FLL}}/a_{\text{ch}}$ but of a much smaller scale.

The observed behavior of the intrachain vortex period a_{ch} particularly its independence of φ and also the proportionality to $1/\sqrt{B_z}$ (or $\propto 1/\sqrt{B_{\text{obs}}}$), effectively rule out that the vortex chains in our crystals (if considered separately from the intervening FLL) could have the same origin as the well-studied vortex chains in YBCO. In other words, neither the presence of the intervening vortex lattice, nor the formation of the vortex chains themselves can be attributed to the anisotropy-induced vortex-vortex attraction considered in Refs. 2–4. The same facts, together with the observation that the vortex periods in the chains and in the FLL have *qualitatively* different dependencies on tilt angle, also rule out the scenario suggested in Ref. 13, i.e., that the chain vortices and the FLL vortices represent two types of attraction-induced chains having different characteristics (different positions of the attractive potential wells and, accordingly, different equilibrium vortex spacings). At the same time, another experimental observation—the maximum in $a_{\text{FLL}}/a_{\text{ch}}$ vs φ —indicates that some property that marks the difference between the chain vortices and the FLL vortices undergoes changes with tilt angle and the two differ most from each other at 70–75° tilt. We suggest that the difference between the two types of vortices lies in their different orientations; that is, the chain vortices are tilted away from the *c* axis *less* than \mathbf{B}_{ext} and the FLL vortices are tilted *more* than \mathbf{B}_{ext} —see inset in Fig. 4. We will now demonstrate that this single assumption allows us to explain consistently all of the observed features of the mixed vortex-chain-FLL phase.

First, an indication that the vortices in our BSCCO crystals may not be parallel to the external field comes from the fact that the observed average magnetic induction at the surface is not equal to the normal component of the applied field at large tilt angles (Fig. 2). One of the boundary conditions for a superconductor in a magnetic field is that the normal component of the field must be continuous at the surface:

$$B_{\text{ext}} \cos \varphi = B \cos \theta, \quad (1)$$

where θ is the tilt angle of the vortices, as the inset in Fig. 2 shows. Then it follows from the observation $B_{\text{obs}} > B_{\text{ext}} \cos \varphi$, for $\varphi \geq 80^\circ$, that $\theta < \varphi$ in this angular in-

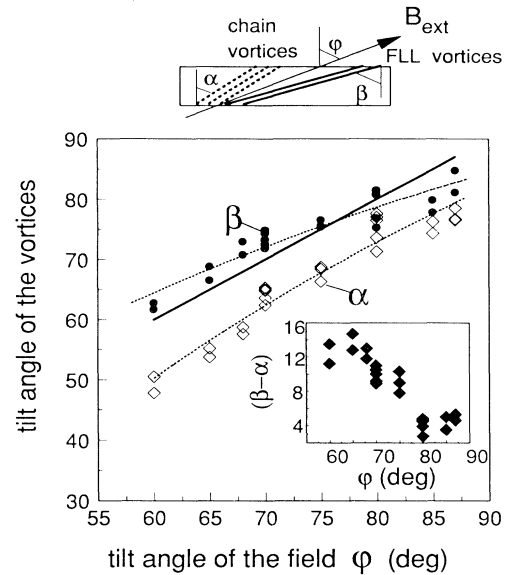


FIG. 4. Calculated values of the tilt angles of the FLL vortices (●) and the chain vortices (◇). The solid line shows corresponding orientations of the external field. The dashed lines are guides to the eye. The inset shows the angular split of the chain and the FLL vortices ($\beta - \alpha$) vs φ .

terval, i.e., the whole ensemble of vortices (on average) is rotated towards the *c* axis in comparison with the external field.

Furthermore, the vortex periods at the surface of the tilted crystal are defined by $B \cos \theta$, i.e., $a = [(2/\sqrt{3})\Phi_0/(B \cos \theta)]^{1/2}$. Therefore, if there are vortices that are tilted less than the average, i.e., at an angle $\alpha < \varphi$, the observed vortex period will be smaller than that corresponding to the average magnetic induction B_z (or B_{obs}); we suggest that these are the chain vortices. If, on the contrary, the vortices are tilted further towards the (*ab*) plane, the observed vortex period will be larger than that corresponding to B_z (or B_{obs}); these are the FLL vortices. According to theory, orientations of the vortices should not depend on the value of the applied field but are defined only by the anisotropy parameter γ , the Ginzburg-Landau parameter κ , and the demagnetization factor.^{10,13} Then the above suggestions, together with an assumption that there is no attractive potential of the type considered in Refs. 2–4, will also explain all the observed field dependencies of a_{ch} , a_{FLL} , and D_{ch} . Furthermore, if the total number of vortices with orientations $\alpha < \varphi$ is less than that of the vortices with orientations $\beta > \varphi$, the most likely arrangement of such two vortex species is a laminar structure, like the one we observe, which accommodates the direction of tilt and the main anisotropy axis *c*. Arranged in this way, the two vortex species will not necessarily have to cross each other in the bulk of the superconductor and one can expect their interaction to be purely via repulsion of their magnetic fields. In fact, one can see in SEM images in Fig. 1 that in the direction perpendicular to the chains, the distance between a chain and the closest FLL row is somewhat

larger than the distance between two adjacent FLL rows. Presumably, the higher density of the chain vortices results in a larger repulsive force on the closest FLL row in comparison with the force from other FLL rows.

Assuming that in each case the change of the vortex period (in comparison with that corresponding to B_z) is due to the rotation of the vortices, we calculate the tilt angles α and β , as follows:

$$\alpha = \arccos \left[\left(\frac{2}{\sqrt{3}} \frac{\Phi_0}{a_{\text{ch}}^2} \right) / B_{\text{ext}} \right], \quad (2)$$

$$\beta = \arccos \left[\left(\frac{2}{\sqrt{3}} \frac{\Phi_0}{a_{\text{FLL}}^2} \right) / B_{\text{ext}} \right]. \quad (3)$$

The results are shown in Fig. 4. One can see that for $\varphi < 80^\circ$, the orientation of the external field lies in between those for the chain and the FLL vortices, the FLL vortices being always orientated very closely to B_{ext} , while the chain vortices deviate substantially from it. For $\varphi = 80^\circ$ we observe mixed behavior: for some crystals, $\beta > \varphi$ and for other $\beta < \varphi$. Finally, for $\varphi = 85^\circ$ and 87° , both the chain and the FLL vortices are always tilted less than the applied field. This result is, of course, in accord with the observation that the average magnetic induction at the sample surface exceeds B_z substantially. As we discuss later, the anomalous behavior for $\varphi \geq 80^\circ$ can be understood if demagnetization effects due to the platelike shape of the crystals are taken into account.

One can notice that the calculated tilt angles, α and β , show considerable spread from sample to sample, well in excess of the deviations over the same sample (the same feature is observed for the data on a_{ch} and, to a less extent, a_{FLL}). Moreover, for $\varphi \geq 80^\circ$, the values of α and β for different crystals overlap so that, if one takes the average over all samples, it is impossible to define the average angular split for the vortex orientations. However, if we plot the difference of the vortex tilt angles, $(\beta - \alpha)$, for every sample, the data looks much clearer, particularly for the largest tilt angles—see inset in Fig. 4. According to theory,^{10,11,13} equilibrium vortex orientations, if they are different from the orientation of the applied field, should be very sensitive to the magnitude of the anisotropy γ . In turn, γ in layered materials like BSCCO is defined by the strength of the Josephson coupling between the adjacent CuO planes.⁸ It follows from a number of experimental studies that high- T_c superconductors, particularly those with a complex crystal structure, like BSCCO, are characterized by considerable differences in Josephson coupling from sample to sample. For example, such an anisotropy-sensitive property as Josephson decoupling in fields nearly parallel to the (ab) plane (the so-called transition to a magnetically transparent state) occurred in two similar crystals of BSCCO,¹⁶ Ta-Ba-Ca-Cu-O (Ref. 17) or Nd-Ce-Cu-O (Ref. 18) at notably different fields. In addition, the transitions in the first two materials were smeared pointing to an inhomogeneous distribution of the Josephson-coupling strengths within the same crystal.^{16,17} Therefore, we believe that

the observed variations of the vortex orientations for the same tilt of the external field must be caused by intrinsic variations of the Josephson coupling from crystal to crystal. In our experiment, we find evidence that the vortex orientations are characteristic of the particular crystal and do not depend on other factors, like the thickness of the sample or slight differences in decoration conditions. In two separate experiments, for $\varphi = 75^\circ$, $B_{\text{ext}} = 75$ G, and $\varphi = 80^\circ$ and $B_{\text{ext}} = 135$ G, we decorated simultaneously a thick crystal, of ≈ 80 – 100 μm thickness, a thin (15 – 20 μm) slice of the same crystal cleaved prior to decoration, and another crystal from the same batch. In both experiments we found that the parameters a_{ch} and a_{FLL} (and, consequently, α and β) were essentially the same for the thick and the thin slices of the same crystal but their values for the third crystal showed noticeably larger differences.

The first test of the proposed explanation for the formation of the coexisting vortex chains and the FLL comes from the obvious requirement that the added partial magnetic fields induced by the chain and the FLL vortices be equal the external field, i.e., $B_{\text{ch}}^p + B_{\text{FLL}}^p = B_{\text{ext}}$ [see inset in Fig. 3(b)]. The partial fields are calculated as $B_{\text{ch}}^p = (N_{\text{ch}} \Phi_0) / \cos \alpha$; $B_{\text{FLL}}^p = (N_{\text{FLL}} \Phi_0) / \cos \beta$; where $N_{\text{ch}} = 1 / (a_{\text{ch}} D_{\text{ch}})$, and $N_{\text{FLL}} = [2 / (\sqrt{3} a_{\text{FLL}}^2)] (1 - a_{\text{ch}} / D_{\text{ch}})$ are the numbers of the chain and FLL vortices per unit area, respectively. We find that the above relation holds to an excellent accuracy for all tilt angles and applied fields. Selected (but typical) examples are shown in Table I. The Table also demonstrates that the boundary condition (1) is fulfilled for $\varphi \leq 80^\circ$; i.e., $\sum B_z^p \approx B_z$, where $\sum B_z^p = B_{\text{ch}}^p \cos \alpha + B_{\text{FLL}}^p \cos \beta$.

A further argument in favor of the two vortex species comes from the following consideration. If the arrangement of the chain and FLL vortices is such as that shown in Fig. 4, the partial magnetic fields, B_{ch}^p and B_{FLL}^p , are uniquely defined by three parameters: B_{ext} and the tilt angles, α and β . In turn, the partial fields define ratios which the numbers of chain and FLL vortices make to the total number of the vortices. In other words, they define the ratios $N_{\text{ch}} / N_{\text{FLL}}$ and $D_{\text{ch}} / a_{\text{FLL}}$. Therefore, we can calculate the number of FLL vortex rows between the chains that one should expect if the chain and the FLL vortices do have different orientations. The tilt angles α and β are the only parameters used in this calculation. By employing simple geometrical arguments, we get

TABLE I. Comparison of the partial magnetic fields due to chain vortices B_{ch}^p and FLL vortices B_{FLL}^p with the applied field B_{ext} (see text for details).

φ	B_z , G	$\sum B_z^p$, G	B_{ext} , G	$\sum B^p$, G
60°	18	17.1	36	35.8
65°	14.6	13.5	35	34.3
70°	6.5	5.8	19	18.8
75°	14.5	15.1	56	55.3
80°	23.4	22.7	135	133.3
85°	9.6	21.1	110	109.5
87°	5.9	19.6	113	112.9

$$\frac{D_{\text{ch}}}{a_{\text{FLL}}} = \frac{\sqrt{3}}{2} \left[\frac{\cos\beta}{\cos\alpha} \right]^{1/2} \frac{\sin(\beta-\alpha)}{\sin(\beta-\varphi)}. \quad (4)$$

The result is shown by the solid line in Fig. 3(b); the values of $a_{\text{FLL}}/a_{\text{ch}}$ used to find α and β are marked by filled symbols in Fig. 3(a). One can see that calculated values of $D_{\text{ch}}/a_{\text{FLL}}$ reproduce rather well the rapid decrease with φ observed in experiment. In addition, it follows from expression (4) that the main factor defining $D_{\text{ch}}/a_{\text{FLL}}$ should be the angular split of the vortices, $(\beta-\alpha)$, since $\sin(\beta-\alpha) \approx (\beta-\alpha)$, $\sin(\beta-\varphi) \approx (\beta-\varphi)$ and the difference $(\beta-\varphi)$ does not change much over the angle interval $60^\circ < \varphi \leq 80^\circ$. It is indeed the case in the experiment as one can see from comparison of Fig. 3(b) and $(\beta-\alpha)$ vs φ dependence shown in the inset in Fig. 4. For the largest tilt angles, $\varphi > 80^\circ$, relation (4) is obviously not valid because of the complications associated with the rotation of the whole vortex ensemble (see above).

Note that in our explanation, the orientations of the vortices differ from those predicted in Ref. 10 (both vortex species tilted much further away from the c axis than \mathbf{B}_{ext}). This discrepancy is perhaps not surprising because the calculations were performed within the anisotropic London theory, which is a simplified description of a weakly coupled superconductor, and in the limit of noninteracting vortices. The more suitable Lawrence-Doniach model, which takes account of the Josephson coupling between the layers, also predicts a ‘‘combined lattice’’ but of a different type. This one should be composed of the vortices parallel to the c axis and parallel to the (ab) plane. It should replace the uniformly tilted FLL when the orientation of \mathbf{B}_{ext} is close to the layers and the perpendicular component of the field starts to penetrate the sample but is still not too large in comparison with $H_{c1,z}$, the first critical field in the direction perpendicular to the layers.⁸ Although the above conditions are satisfied in our experiments, the data clearly reject the existence of two sets of mutually perpendicular vortices.

Finally, the ‘‘anomalous’’ orientations of the vortices for $\varphi \geq 80^\circ$ can be understood when demagnetization effects due to the slablike shape of the crystals are considered.^{13,19} In this case, even for not too thin slabs of an anisotropic superconductor (of thickness $d \gg \lambda$) placed in low magnetic fields, $B_z \leq H_{c1}$, the slope of the vortices should fall below the slope of the applied field. Namely, if the slope of the external field $\mathbf{B}_{\text{ext}} = (B_s, 0, B_z)$ is $t_s = B_s/B_z$; the slope of the vortices should be¹⁹

$$t(\varphi) = t_s(\varphi) (\pi\lambda/a)^2 / [\gamma^{-2} \ln(\gamma\kappa) + \frac{1}{2}]. \quad (5)$$

For the anisotropy parameter $\gamma = 150$ (Ref. 20) and the GL parameter $\kappa = 60$, corresponding slopes $t(\varphi)$ and $t_s(\varphi)$ are shown in Fig. 5. Clearly, the shape factor leads to more ‘‘vertical’’ orientations of the vortices. Moreover, expected misorientation of the vortex slopes away from \mathbf{B}_{ext} should become larger for the largest tilt angles that can explain our observation of the anomalous vortex orientations for $\varphi \geq 80^\circ$ only.

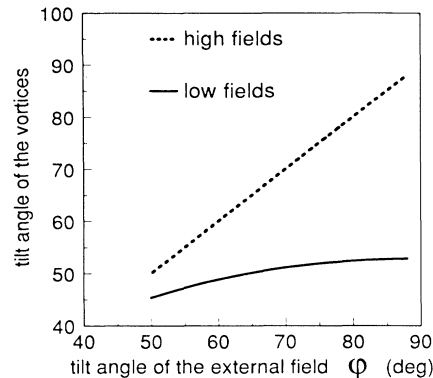


FIG. 5. Deviations of the vortex orientations (tilt angles) from the orientations of the external field calculated for a slab-shaped superconducting crystal using expression (5). In high fields, $B_z \gg H_{c1}$, the vortices should be parallel to \mathbf{B}_{ext} (dashed line). In low fields $B_z < H_{c1}$, the orientations of the vortices (solid line) differ from those of the external field (dashed line).

CONCLUSIONS

We report a detailed study of the mixed vortex phase found in highly anisotropic BSCCO-2212 in tilted magnetic fields. The vortex structure consists of dense vortex chains running parallel to the (\mathbf{B}, c) plane, and the intervening hexagonal vortex lattice. The presence of the intervening FLL is contradictory to the well-studied vortex-chain phase found in moderately anisotropic YBCO (the latter is well-described by the anisotropic London theory).

Due to the very high quality of our crystals we were able to find systematic dependencies on tilt angle of the parameters of this unusual vortex structure which indicated its anisotropy-related nature. Proceeding from these dependencies, we demonstrate that the formation of this new vortex phase can be understood if one assumes that the chain and the FLL vortices represent two vortex species having different orientations in the crystal: for tilt angles of the applied field $\varphi < 80^\circ$, the chain vortices are tilted less than the applied field, at an angle $\alpha < \varphi$, while the FLL vortices are tilted more, at an angle $\beta > \varphi$. For $\varphi \geq 80^\circ$, an additional demagnetization effect due to the slablike shape of the crystals becomes important and leads to both the chain and the FLL vortices being tilted further away from the (ab) plane than the external field. The possibility of such a split of the tilted vortex lattice into two species for superconductors with extreme anisotropies was suggested by recent theoretical calculations.

The tilt angle and field dependencies of the vortex period in the chains in BSCCO are found to be qualitatively different from those in moderately anisotropic YBCO. Therefore, we conclude that the attractive interaction between the vortices, of the type found in YBCO crystals, cannot account for the origin of the vor-

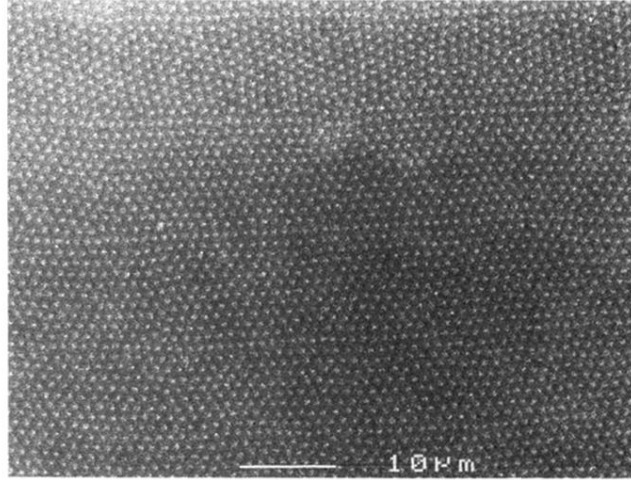
tex chains in BSCCO even if the latter are considered separately from the intervening FLL. However, we would like to emphasize that a possibility cannot be ruled out that, in addition to the split of the tilted vortex lattice into two species, there exists an attractive interaction between the chain vortices of some other, yet unknown, type.

ACKNOWLEDGMENTS

We would like to thank V. G. Kogan, L. N. Bulaevskii, A. I. Buzdin, W. Barford, and M. Moore for helpful discussions. This work was supported by the Engineering and Physical Sciences Research Council of the United Kingdom.

-
- ¹L. J. Campbell, M. M. Doria, and V. G. Kogan, *Phys. Rev. B* **38**, 2439 (1988); A. M. Grishin, A. Yu. Martynovich, and S. V. Yampolskii, *Sov. Phys. JETP* **74**, 345 (1992).
- ²A. I. Buzdin and A. Yu. Simonov, *Physica C* **168**, 421 (1990).
- ³A. M. Grishin, A. Yu. Martynovich, and S. V. Yampolskii, *Sov. Phys. JETP* **70**, 1089 (1990).
- ⁴L. L. Daemen, L. J. Campbell, and V. G. Kogan, *Phys. Rev. B* **46**, 3631 (1992).
- ⁵B. I. Ivlev and N. B. Kopnin, *Phys. Rev. B* **44**, 2747 (1991).
- ⁶P. L. Gammel *et al.*, *Phys. Rev. Lett.* **68**, 3343 (1992).
- ⁷I. V. Grigorieva, J. W. Steeds, and K. Sasaki, *Phys. Rev. B* **48**, 16 865 (1993).
- ⁸L. N. Bulaevskii, M. Ledvij, and V. G. Kogan, *Phys. Rev. B* **46**, 366 (1992); D. A. Huse, *ibid.* **46**, 8621 (1992).
- ⁹L. L. Daemen *et al.*, *Phys. Rev. Lett.* **70**, 2948 (1993).
- ¹⁰A. Sudbo, E. H. Brandt, and D. A. Huse, *Phys. Rev. Lett.* **71**, 1451 (1993).
- ¹¹E. Sardella and M. Moore, *Phys. Rev. B* **48**, 9664 (1993).
- ¹²C. A. Bolle *et al.*, *Phys. Rev. Lett.* **66**, 112 (1991).
- ¹³A. Yu. Martynovich, *JETP* **78**, 489 (1994).
- ¹⁴G. Balakrishnan, D. Mck. Paul, M. R. Lees, and A. T. Boothroyd, *Physica C* **206**, 148 (1993).
- ¹⁵I. V. Grigorieva, L. A. Gurevich, and L. Ya. Vinnikov, *Physica C* **195**, 327 (1992).
- ¹⁶N. Nakamura, G. D. Gu, and N. Koshizuka, *Phys. Rev. Lett.* **71**, 915 (1993).
- ¹⁷F. Zuo *et al.*, *Phys. Rev. B* **49**, 9252 (1994).
- ¹⁸F. Zuo *et al.*, *Phys. Rev. Lett.* **72**, 1746 (1994).
- ¹⁹E. H. Brandt, *Phys. Rev. B* **48**, 6699 (1993).
- ²⁰J. C. Martínez *et al.*, *Phys. Rev. Lett.* **69**, 2276 (1992).

(a)



(b)

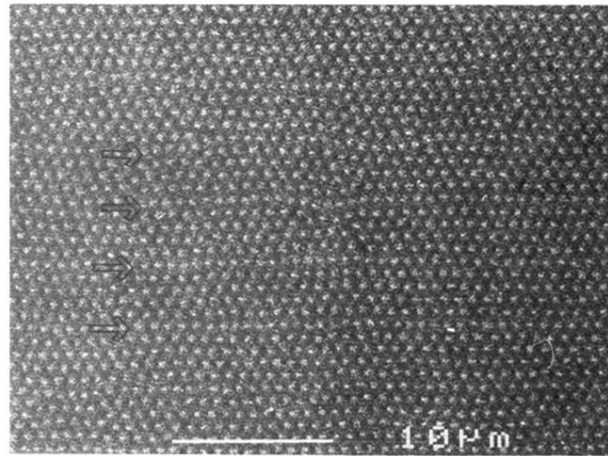


FIG. 1. SEM images of the mixed vortex-chain-FLL phase. (a) The tilt angle of the external field $\varphi=60^\circ$. (b) $\varphi=80^\circ$. The projections of the (\mathbf{B}, \mathbf{c}) plane on the sample surface are horizontal. Since the vortex chains in Fig. 1(b) are not seen very easily, few of them are marked by the arrows.